PRENATAL DIAGNOSIS
Prenat Diagn 2005; **25**: 442–447.
Published online in Wiley InterScience (www.interscience.wiley.com). **DOI:** 10.1002/pd.1145

SHORT COMMUNICATION

Prenatal diagnosis in pregnancies at risk for Joubert syndrome by ultrasound and MRI

Dan Doherty[1]*, Ian A. Glass[1,2], Joseph R. Siebert[1], Peter J. Strouse[3], Melissa A. Parisi[1], Dennis W. W. Shaw[4], Phillip F. Chance[1,5], Mason Barr Jr[6] and David Nyberg[7]

[1]*University of Washington/Children's Hospital and Regional Medical Center, Department of Pediatrics, Seattle, WA, USA*
[2]*University of Washington Department of Medicine, Seattle, WA, USA*
[3]*University of Michigan Department of Radiology, Ann Arbor, MI, USA*
[4]*University of Washington Department of Radiology, Seattle, WA, USA*
[5]*University of Washington Department of Neurology, Seattle, WA, USA*
[6]*University of Washington Department of Pediatrics, Seattle, WA, USA*
[7]*Fetal and Women's Center of Arizona, Phoenix, AZ, USA*

Objectives To describe the prenatal imaging findings in fetuses at risk for Joubert syndrome (JS), review the literature and propose a protocol for prenatal diagnosis of JS using ultrasound and MRI.

Methods We reviewed prenatal ultrasound and fetal MRI studies in two pregnancies at 25% recurrence risk for JS and correlated these findings with gross neuropathology in one affected fetus.

Results While abnormalities such as occipital encephalocele or enlarged cisterna magna have been identified before mid-trimester, the definitive diagnosis of JS, based on core cerebellar findings, has only been possible after 17 weeks' gestation.

Conclusions With longitudinal monitoring, it is possible to diagnose JS in at-risk pregnancies before 24 weeks' gestation. On the basis of our data and review of the literature, we propose a protocol for monitoring pregnancies at risk for JS, utilizing serial ultrasounds combined with fetal MRI at 20–22 weeks' gestation to maximize the accuracy of prenatal diagnosis. Copyright © 2005 John Wiley & Sons, Ltd.

KEY WORDS: Joubert syndrome; prenatal diagnosis; ultrasound; fetal MRI; pathology

INTRODUCTION

Joubert *et al*. (1969) described four siblings with 'episodic hyperpnea, abnormal eye movements, ataxia and mental retardation' associated with agenesis of the cerebellar vermis and inherited in an autosomal recessive manner. Since that initial report, more than one hundred cases of Joubert syndrome (JS [MIM 213300]) have been described in the medical literature. These reports have confirmed the original findings and established the 'molar tooth sign' (MTS) as the cardinal diagnostic imaging feature (Maria *et al*., 1997, 1999a). The MTS is visualized on axial brain MRI and results from the combination of a hypoplastic cerebellar vermis, elongated and thickened superior cerebellar peduncles and a deep interpeduncular fossa. Retinal dystrophy, retinal coloboma, polydactyly, occipital encephalocele, oral frenulae, liver fibrosis and kidney disease are also seen in some patients (Boltshauser and Isler, 1977; Joubert *et al*., 1969; Maria *et al*., 1999b; Parisi and Glass, 2003; Saraiva and Baraitser, 1992). These variable findings have led to more recent broader classifications including 'cerebello-oculo-renal syndromes' (CORS) and 'Joubert syndrome and related disorders' (JSRD; Gleeson *et al*., 2004; Keeler *et al*., 2003). The exact configuration of the cerebellum and brainstem can vary significantly even between identical twins (Quisling *et al*., 1999; Raynes *et al*., 1999). The prognosis for patients with JS is also highly variable: some patients die in infancy, some are non-ambulatory and non-verbal, and others can walk without assistance and communicate using well-formed sentences (Steinlin *et al*., 1997).

In addition to the clinical heterogeneity of JS, mutations in two genes (*NPHP1* and *AHI1*) have been implicated in subsets of patients with JS (Dixon-Salazar *et al*., 2004; Ferland *et al*., 2004; Parisi *et al*., 2004). These two genes are estimated to account for less than 20% of cases (Parisi, unpublished data). Two other loci have been mapped to large intervals at chromosome 9q34.3 and the pericentromeric region of chromosome 11 (Keeler *et al*., 2003; Saar *et al*., 1999; Valente *et al*., 2003). Despite these advances, clinical genetic testing for JS is not routinely available; however, *NPHP1* mutation testing is available in several clinical laboratories for patients with a specific form of renal disease (nephronophthisis).

*Correspondence to: Dan Doherty, University of Washington/Children's Hospital and Regional Medical Center, Department of Pediatrics, Seattle, WA, USA.
E-mail: ddoher@u.washington.edu

Received: 3 December 2004
Revised: 1 March 2005
Accepted: 8 March 2005

Thus, parents of a child with JS have a 25% chance of conceiving an affected fetus with each pregnancy, and, for the majority, no definitive prenatal testing is available to aid with reproductive planning.

Given the low prevalence of JS (~1/100 000 live births) and the non-specific nature of many of the ultrasound (US) findings, *in utero* diagnosis of JS has been problematic, especially early in pregnancy. Normal values for cisterna magna and vermis dimensions by prenatal US have been described (Mahony *et al*., 1984; Serhatlioglu *et al*., 2003; Zalel *et al*., 2002); however, there is a range of normal values and it may be difficult to distinguish normal from abnormal, especially before 18 weeks when the cerebellar vermis is still developing (Bromley *et al*., 1994). The term 'Dandy–Walker Variant' has been used for vermis hypoplasia without a large posterior fossa cyst or hydrocephalus in patients who do not fit a more specific diagnosis (Nyberg *et al*., 1988). This term is non-specific, includes a variety of underlying causes and likely overlaps with Dandy–Walker malformation (Barkovich *et al*., 1989; Nyberg *et al*., 1991, 2002). Finally, postnatal imaging and fetal post-mortem examination do not always confirm posterior fossa prenatal US findings (Carroll *et al*., 2000; Laing *et al*., 1994).

In this report, we describe prenatal imaging (both US and MRI) of two fetuses at risk for JS, one affected and one unaffected. In addition, we review the literature and discuss the implications for evaluation and management of at-risk pregnancies.

Case 1

A G4 P2 SAB1 woman who had previously given birth to a child with JS underwent prenatal monitoring for JS. The prior affected child manifested developmental delay, hypotonia, ataxia, nystagmus, oculomotor apraxia, strabismus, bilateral ptosis and rhythmic tongue protrusion. The child did not have an encephalocele, polydactyly, retinal colobomas, retinal dystrophy, renal dysfunction or any of the other variable findings of JS. The child had normal vision, a normal electroretinogram and structurally normal kidneys on US at 4 years of age. An MRI at 1 month of age revealed the MTS, confirming the diagnosis of JS (Figure 1). At 5 years of age, the child could sit, but not crawl or walk, and was interactive, using one sign to communicate.

Family history: Parents are unrelated, healthy and of northern European descent. In addition to the affected sibling described above, there is another, unaffected, healthy sibling. There is no other family history of neurologic, genetic or developmental problems.

Pregnancy history: This pregnancy was uneventful, without maternal fevers or exposures. Mother received close prenatal care.

Imaging findings: No extracranial abnormalities were identified on transabdominal US examinations at 13 5/7, 16 and 20 5/7 weeks' gestation. In particular, amniotic fluid volume was normal and no renal cysts or polydactyly were observed. Fetal measurements were consistent with dates by last menstrual period, although head measurements were in the upper range of normal. Nuchal translucency measurement was normal (less than 2 mm at 13 5/7 and 16 weeks' gestation). No abnormal fetal movements or abnormal breathing pattern were reported.

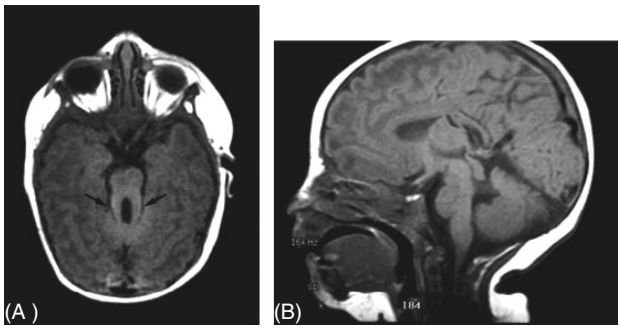

Figure 1—MRI of Case 1 older sibling with Joubert syndrome at 1 month of age. (A) Axial view: thick, elongated superior cerebellar peduncles, the deep interpeduncular fossa is visible in an adjacent slice. (B) Midline sagittal view: abnormal configuration of the 4th ventricle, the hypoplastic vermis is difficult to distinguish from the cerebellar hemispheres impinging on the midline slice

The 16-week US revealed an apparent fluid connection between the fourth ventricle and the cisterna magna at the inferior aspect of the cerebellum. A repeat US at 20 5/7 weeks showed prominence of the cisterna magna (9 mm), although the measurement remained within normal range (<10 mm). While the superior vermis appeared intact (Figure 2A), a 'key hole' communication between the fourth ventricle and cisterna magna was more clearly apparent (Figure 2B), and the US was interpreted as abnormal. Of note, the transcerebellar diameter was normal. All USs were performed using a Philips HDI 5000 System (Philips Medical Systems, Bothell, WA) and standard techniques (Nyberg *et al*., 2002).

Magnetic resonance imaging was performed at 21 weeks' gestation. Axial views revealed an enlarged cisterna magna in communication with the 4th ventricle (Figure 3A, C), confirming the US findings. A typical MTS was not seen on axial views, but there was some suggestion of deepening of the interpeduncular fossa (not shown). In the mid-sagittal view, the vermis was very small and rostrally located (Figure 3E). The cerebellar hemispheres and supratentorial structures appeared normal in all views. MRI images were acquired using a 1.5-T Signa Genesis System (General Electric, Milwaukee, WI, USA). Single-shot fast spine echo (FSE) sequences were used to obtain axial (TR: ~6000,

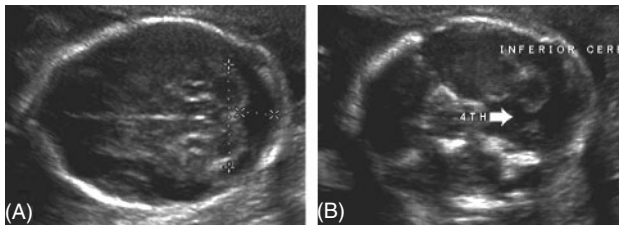

Figure 2—Prenatal ultrasound of affected fetus (Case 1) at 21 weeks' gestation. (A) Superiorly, the midline cerebellum appears intact. (B) Inferiorly, an apparent connection between the 4th ventricle and cisterna magna is present (white arrow)

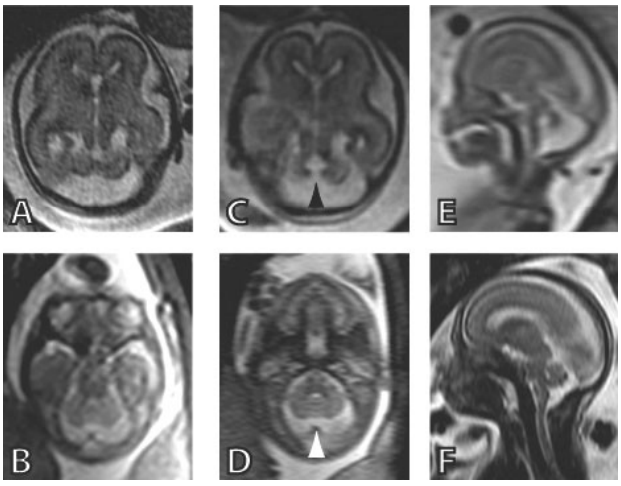

Figure 3—Fetal MRI of affected fetus (Case 1) at 21 EGA(A,C,E) and unaffected fetus (Case 2) 22 weeks EGA (B,D,F). (A–B) Superiorly, the midline cerebellum appears intact in both Case 1 (A) and Case 2 (B). (C–D) Inferiorly, a connection between the 4th ventricle and cisterna magna is apparent in the affected Case 1 (black arrowhead in C), but not in unaffected Case 2 (white arrowhead in D). (E–F) In midline sagittal views, Case 1 demonstrates a small vermis and above average size cisterna magna (E), versus the normal structures in Case 2 (F). Less cerebral cortex is visualized in (B,D) because the plane of section is more horizontal than in (A,C). EGA = estimated gestational age. See text for details of MRI acquisition

TE: ~100), sagittal (TR: 1159, TE: 100) and coronal (TR: ~6000, TE: ~100) views (Coakley *et al*., 2004). Slice thickness ranged from 4–5 mm with 0–2 mm between slices.

Post-mortem examination: The pregnancy was electively terminated at 22 3/7 weeks' gestation and a post-mortem examination was performed. The male fetus displayed gestationally appropriate measurements and normal external features except for an OFC that was 2.3 SD above the mean, mild pectus excavatum, telecanthus (inner canthal distance 18.2 mm, >2 SD for gestational age) and a single palmar crease on the right hand. There was no polydactyly. The tongue was normal without evidence of masses or abnormal frenulae and the kidneys and liver appeared grossly normal.

The neuropathological examination revealed normal supratentorial structures with generous extra-axial fluid, but no ventriculomegaly. A recent intraventricular hemorrhage was evident, likely occurring at the time of termination. The tentorium was not elevated. No large posterior fossa fluid collection was found. The brainstem appeared normal on gross examination. No cerebellar vermis was present inferiorly; however, a very small remnant of dysplastic midline tissue was present superiorly. The cerebellar hemispheres and folia were angled upward toward the midline in an inverted V shape (Figure 4A).

Case 2

We reviewed the 19.5-week US and 22-week MRI of an unrelated at-risk fetus. MRI images were acquired using a 1.5-T Magnetom Symphony System (Siemens, Erlangen, Germany). T2 HASTE sequences with fat saturation

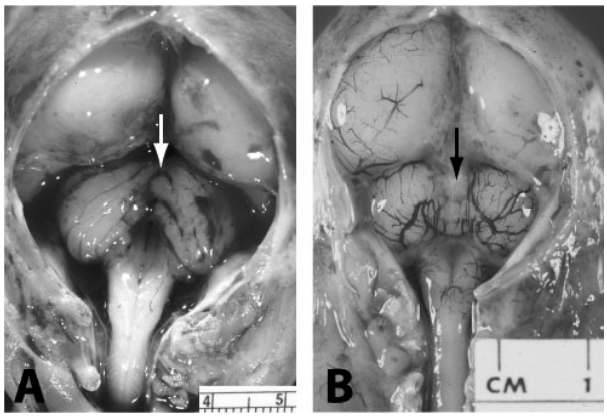

Figure 4—Posterior fossa *in situ*. (A) 22-week gestation fetus with JS demonstrating deficient vermis (white arrow) and large opening to the 4th ventricle. (B) For comparison: 20-week gestation fetus with intact vermis (black arrow) and small opening to the 4th ventricle. Note that the meninges have been removed in A but not B. The fetus in (B) was born spontaneously due to chorioamnionitis and probably placental abruption. Prenatal ultrasounds were normal at 13 and 18 *abruptio*. Prenatal ultrasounds were normal at 13 and 18 weeks' gestation

(TR: 1900, TE: 170) were used to obtain axial, sagittal and coronal views. Slice thickness ranged from 4–5 mm with 0 mm between slices. Similar to Case 1, one older sibling has JS with abnormal eye movements, hypotonia, abnormal breathing pattern and developmental delay, and another older sibling is unaffected. Prenatal imaging studies were completely normal (Figure 3B, D and F), predicting an unaffected child. A healthy girl was born at 39 weeks' gestation without complications.

DISCUSSION

Case 1 provides the first combined description of serial prenatal USs, fetal MRI and pathological findings in a fetus ultimately diagnosed with JS. Thus far, prenatal diagnosis of JS has proved difficult because of the relatively non-specific prenatal US findings reported in most affected fetuses. Table 1 summarizes the imaging findings seen in the published case reports of fetuses with JS. Including our case with the ten fetuses reported in the literature, six were noted to have vermis hypoplasia, four an enlarged cisterna magna, four an occipital encephalocele, two an increased nuchal translucency, and one each polydactyly, renal cysts, ventriculomegaly, polyhydramnios or hypoplastic phallus. It is not possible to estimate the frequency of prenatal US findings in fetuses with JS because the published reports describe highly selected cases, apply variable criteria for vermis hypoplasia/enlarged cisterna magna or do not report all prenatal US findings in all cases. Each of these findings can be seen in other disorders making definitive prenatal diagnosis difficult in the absence of a family history. For couples with an affected child, prenatal diagnosis of JS is less problematic. It is exceedingly unlikely that features such as enlarged cisterna magna, vermis hypoplasia, encephalocele or polydactyly will be present in a subsequent pregnancy simply by chance. Our Case 1 manifested only vermis hypoplasia, without any other findings.

Table 1—Summary of JS prenatal diagnosis case reports

Reference	FHx	Sex	Initial findings	Age at diagnosis	Confirmed by	Outcome
Present study	+	M	17 weeks: CVH	17 weeks' gestation	FH plus *in utero* US/MRI plus post-mortem (CVH)	TAB 22 weeks
(Campbell *et al*., 1984)	+	F	21 weeks: ECM	26 weeks' gestation	FH plus post-mortem (CVH)	TAB 26 weeks
(Ivarsson *et al*., 1993)	+	ND	17 weeks: OE, REN	17 weeks' gestation	FH plus OE, REN	TAB ~17 weeks
(van Dorp *et al*., 1991)	+	F	17 weeks: OE, ECM, CVH	17 weeks' gestation	FH plus post-mortem (CVH, OE, cb dysplasia, coloboma)	TAB 17 weeks
(van Zalen-Sprock *et al*., 1996)	+	ND	8–11 weeks: ECM, OE	Before birth	FH plus ECM, OE plus post-mortem (no details)	TAB
(Wang *et al*., 1999)	+	M	32 weeks: CVH, OE	32 weeks' gestation	FH plus OE plus post-mortem (OE, CVH)	TAB 32 weeks
(Aslan *et al*., 2002)	CSG	M	32 weeks: PH, CVH, VM, PD, RESP	32 weeks' gestation	Fetal US[a] and MTS on postnatal MRI	Liveborn
(Anderson *et al*., 1999)	—	F	18 weeks: normal	Birth	CVH and VM on MRI, clinical features[b]	Alive at 5 weeks
(Ni Scanaill *et al*., 1999)	—	F	24 weeks: CVH, ECM	Infancy	CT scan, clinical features[c]	Alive at 16 months
(Reynders *et al*., 1997)	—	ND	13.5 weeks: NT	ND	ND	Liveborn
(Souka *et al*., 1998)	—	ND	11 weeks: NT; 20 weeks CVH	ND (after 20 weeks' gestation)	ND	TAB

CSG, consanguineous; CVH, cerebellar vermis hypoplasia; ECM, enlarged cisterna magna; FH, family history; ND, not documented; NT, increased nuchal translucency; OE, occipital encephalocele; PD, polydactyly; PH, polyhydramnios; REN, renal cysts; RESP, abnormal breathing; TAB, therapeutic abortion; US, ultrasound; VM, ventriculomegaly.

[a] After birth, the child displayed the molar tooth sign, hypotonia, polydactyly, tongue hamartomas, apnea/tachypnea, nystagmus and retinal dystrophy.

[b] After birth, the child displayed VM requiring shunting, minor polar cataracts, Leber's congenital amaurosis, the molar tooth sign, mild hypotonia, apnea/tachypnea, nystagmus.

[c] After birth, the child displayed multicystic renal disease, eye movement abnormalities, impaired vision, panting respirations, truncal hypotonia.

Successful prenatal diagnosis of JS based on brain imaging findings is dependent on demonstrating vermis hypoplasia, usually affecting the inferior vermis. Vermis hypoplasia appears as a fluid communication between the fourth ventricle and the cisterna magna that persists after 18 weeks' gestation. Potential false-positive diagnoses may occur by scanning too early (before 18 weeks) when the vermis may not yet cover the fourth ventricle (Bromley *et al*., 1994), or by scanning just below the level of the cerebellar hemispheres, giving the erroneous impression of vermian agenesis or hypoplasia (Babcook *et al*., 1996). A further limitation of prenatal US is the difficulty in obtaining sagittal views due to fetal orientation. Three-dimensional multiplanar US may be helpful in obtaining sagittal views, although its efficacy in diagnosing vermian defects has not been proven.

Prenatal MRI can be very helpful in the diagnosis of posterior fossa abnormalities (Adamsbaum *et al*., 2005; Levine *et al*., 2003). Advantages of MRI over US include superior tissue discrimination and resolution, elimination of US artifacts and the ability to achieve multiple planes of imaging including sagittal views regardless of fetal positioning. The developing calvaria can limit US visualization of the brain, but does not hinder visualization by MRI. Fetal MRI has the potential to identify the MTS, but the MTS was not visible at 20 weeks' gestation in Case 1. It is possible that the MTS is not yet present at this gestational age; however, it is also possible that the particular MRI slices in this case did not capture the MTS.

On the basis of the normal development of the hindbrain, the available case reports and our experience, we propose the following sequence of evaluations for at-risk pregnancies (Table 2). The purpose of the 11- to 14-week US is to evaluate for increased nuchal translucency. The 16-, 18- and 20-week USs serve to monitor the vermis for growth and provide multiple opportunities to detect the other features associated with JS. Fetal MRI at 20–22 weeks' gestation represents the final opportunity to detect posterior fossa abnormalities or confirm normal anatomy prior to constraints on reproductive choices in the United States. If possible, these imaging studies should be reviewed by a radiologist, perinatologist or obstetrician with specific experience in the diagnosis of posterior fossa malformations. Further imaging or other evaluations may be indicated, based on the unique circumstances of each pregnancy. Note that with a known family history of JS, a karyotype is necessary only if one was not performed on the first affected child, or if the first child's karyotype was abnormal. Although *NPHP1* mutations are a rare cause of JS, *NPHP1* DNA testing should be considered if the first child was not tested, especially if there is a family history of renal disease or if the first child had an *NPHP1* mutation. Genetic testing for mutations in other genes such as *AHI1* may be available in the near future. Given the rapid advances in genetic research, referral to a geneticist could be considered.

Depending on the gestational age at diagnosis, the couple may have the option to terminate the pregnancy and should be counseled accordingly. Autopsy is of great value to confirm the diagnosis. For pregnancies that continue, serial USs should be considered to monitor for ventriculomegaly, polyhydramnios and fetal growth. Otherwise, routine obstetrical care is sufficient. Pediatric resuscitation and ICU care should be available at the birth hospital in case the infant has severe apnea in the perinatal period.

Table 2—Recommendations for evaluation of pregnancies at risk for JS

Gest. age	Evaluation	Findings of interest
11–12 weeks	US	Dates, nuchal translucency measurement
16 weeks	US	Full anatomic survey, close examination of the posterior fossa, cisterna magna measurement, evaluation for encephalocele, polydactyly, kidney abnormalities.
<18 weeks	Karyotype	If not performed on previous affected child.
<18 weeks	DNA testing	Only if previous affected child was positive or testing was not performed.
18 weeks	US	Vermis measurements (height, diameter), re-examination of posterior fossa, cisterna magna measurement, reevaluation for encephalocele, polydactyly, kidney abnormalities.
20 weeks	US	Vermis measurements (height, diameter), reexamination of posterior fossa, cisterna magna measurement, reevaluation for encephalocele, polydactyly, kidney abnormalities. May include 3D US.
20–22 weeks	MRI	Evaluation for supratentorial abnormalities and confirmation of posterior fossa findings from US.

Ventriculomegaly, abnormal breathing, micropenis and polyhydramnios have also been reported in fetuses with JS.

It is clear that the *in utero* diagnosis of JS and other posterior fossa malformation syndromes continues to be problematic. The positive and negative predictive value of prenatal imaging findings for the diagnosis of JS is not yet known. Improving on the current state of the art will require multiple approaches. Retrospective review of the prenatal imaging studies on patients known to have JS may provide additional clues to the appearance of posterior fossa structures in fetuses with JS during development. Prospective studies correlating prenatal imaging findings with long-term outcomes will be essential to provide adequate information for counseling families in the future. Results from these studies will inform future research to develop reliable methods for prenatal diagnosis of other hindbrain malformations.

ACKNOWLEDGEMENTS

We thank the families described in this report for their willingness to share their experience. We also

thank Raj Kapur, MD for his helpful comments on the pathology and the manuscript. Dr Doherty is supported by the University of Washington Leadership Education in Neurodevelopmental and Related Disabilities grant (T73MC00041-14-01) from the Maternal and Child Health Bureau, Health Resources and Services Administration, DHHS.

REFERENCES

Adamsbaum C, Moutard ML, Andre C, *et al*. 2005. MRI of the fetal posterior fossa. *Pediatr Radiol* **35**: 124–140.

Anderson JS, Gorey MT, Pasternak JF, Trommer BL. 1999. Joubert's syndrome and prenatal hydrocephalus. *Pediatr Neurol* **20**: 403–405.

Aslan H, Ulker V, Gulcan EM, *et al*. 2002. Prenatal diagnosis of Joubert syndrome: a case report. *Prenat Diagn* **22**: 13–16.

Babcook CJ, Chong BW, Salamat MS, Ellis WG, Goldstein RB. 1996. Sonographic anatomy of the developing cerebellum: normal embryology can resemble pathology. *AJR Am J Roentgenol* **166**: 427–433.

Barkovich AJ, Kjos BO, Norman D, Edwards MS. 1989. Revised classification of posterior fossa cysts and cystlike malformations based on the results of multiplanar MR imaging. *Am J Roentgenol* **153**: 1289–1300.

Boltshauser E, Isler W. 1977. Joubert syndrome: episodic hyperpnea, abnormal eye movements, retardation and ataxia, associated with dysplasia of the cerebellar vermis. *Neuropediatrie* **8**: 57–66.

Bromley B, Nadel AS, Pauker S, Estroff JA, Benacerraf BR. 1994. Closure of the cerebellar vermis: evaluation with second trimester US. *Radiology* **193**: 761–763.

Campbell S, Tsannatos C, Pearce JM. 1984. The prenatal diagnosis of Joubert's syndrome of familial agenesis of the cerebellar vermis. *Prenat Diagn* **4**: 391–395.

Carroll SG, Porter H, Abdel-Fattah S, Kyle PM, Soothill PW. 2000. Correlation of prenatal ultrasound diagnosis and pathologic findings in fetal brain abnormalities. *Ultrasound Obstet Gynecol* **16**: 149–153.

Coakley FV, Glenn OA, Qayyum A, Barkovich AJ, Goldstein R, Filly RA. 2004. Fetal MRI: a developing technique for the developing patient. *AJR Am J Roentgenol* **182**: 243–252.

Dixon-Salazar T, Silhavy JL, Marsh SE, *et al*. 2004. Mutations in the AHI1 gene, encoding jouberin, cause Joubert syndrome with cortical polymicrogyria. *Am J Hum Genet* **75**: 979–987.

Ferland RJ, Eyaid W, Collura RV, *et al*. 2004. Abnormal cerebellar development and axonal decussation due to mutations in AHI1 in Joubert syndrome. *Nat Genet* **36**: 1008–1013.

Gleeson JG, Keeler LC, Parisi MA, *et al*. 2004. Molar tooth sign of the midbrain-hindbrain junction: occurrence in multiple distinct syndromes. *Am J Med Genet* **125A**: 125–134; discussion 117.

Ivarsson SA, Bjerre I, Brun A, Ljungberg O, Maly E, Taylor I. 1993. Joubert syndrome associated with leber amaurosis and multicystic kidneys. *Am J Med Genet* **45**: 542–547.

Joubert M, Eisenring JJ, Robb JP, Andermann F. 1969. Familial agenesis of the cerebellar vermis. A syndrome of episodic hyperpnea, abnormal eye movements, ataxia, and retardation. *Neurology* **19**: 813–825.

Keeler LC, Marsh SE, Leeflang EP, *et al*. 2003. Linkage analysis in families with Joubert syndrome plus oculo-renal involvement identifies the CORS2 locus on chromosome 11p12-q13.3. *Am J Hum Genet* **73**: 656–662.

Laing FC, Frates MC, Brown DL, Benson CB, Di Salvo DN, Doubilet PM. 1994. Sonography of the fetal posterior fossa: false appearance of mega-cisterna magna and Dandy-Walker variant. *Radiology* **192**: 247–251.

Levine D, Barnes PD, Robertson RR, Wong G, Mehta TS. 2003. Fast MR imaging of fetal central nervous system abnormalities. *Radiology* **229**: 51–61.

Mahony BS, Callen PW, Filly RA, Hoddick WK. 1984. The fetal cisterna magna. *Radiology* **153**: 773–776.

Maria BL, Boltshauser E, Palmer SC, Tran TX. 1999a. Clinical features and revised diagnostic criteria in Joubert syndrome. *J Child Neurol* **14**: 583–590; discussion 590–591.

Maria BL, Quisling RG, Rosainz LC, *et al*. 1999b. Molar tooth sign in Joubert syndrome: clinical, radiologic, and pathologic significance. *J Child Neurol* **14**: 368–376.

Maria BL, Hoang KB, Tusa RJ, *et al*. 1997. "Joubert syndrome" revisited: key ocular motor signs with magnetic resonance imaging correlation. *J Child Neurol* **12**: 423–430.

Ni Scanaill S, Crowley P, Hogan M, Stuart B. 1999. Abnormal prenatal sonographic findings in the posterior cranial fossa: a case of Joubert's syndrome. *Ultrasound Obstet Gynecol* **13**: 71–74.

Nyberg DA, McGahan JP, Pretorius DH, Pilu G. 2002. *Diagnostic Imaging of Fetal Anomalies* (2nd edn), Lippincott Williams & Wilkins: Philadelphia.

Nyberg DA, Cyr DR, Mack LA, Fitzsimmons J, Hickok D, Mahony BS. 1988. The Dandy-Walker malformation prenatal sonographic diagnosis and its clinical significance. *J Ultrasound Med* **7**: 65–71.

Nyberg DA, Mahony BS, Hegge FN, Hickok D, Luthy DA, Kapur R. 1991. Enlarged cisterna magna and the Dandy-Walker malformation: factors associated with chromosome abnormalities. *Obstet Gynecol* **77**: 436–442.

Parisi MA, Glass IA. 2003. *Joubert syndrome. In GeneReviews at GeneTests-GeneClinics: Medical Genetics Information Resource [database online]*. Copyright, University of Washington, Seattle 1997–2003. Available at http://wwwgeneclinicsorg or http://www genetestsorg.

Parisi MA, Bennett CL, Eckert ML, *et al*. 2004. The NPHP1 gene deletion associated with juvenile nephronophthisis is present in a subset of individuals with Joubert syndrome. *Am J Hum Genet* **75**: 82–91.

Quisling RG, Barkovich AJ, Maria BL. 1999. Magnetic resonance imaging features and classification of central nervous system malformations in Joubert syndrome. *J Child Neurol* **14**: 628–635; discussion 669–672.

Raynes HR, Shanske A, Goldberg S, Burde R, Rapin I. 1999. Joubert syndrome: monozygotic twins with discordant phenotypes. *J Child Neurol* **14**: 649–654;discussion 669–672.

Reynders CS, Pauker SP, Benacerraf BR. 1997. First trimester isolated fetal nuchal lucency: significance and outcome. *J Ultrasound Med* **16**: 101–105.

Saar K, Al-Gazali L, Sztriha L, *et al*. 1999. Homozygosity mapping in families with Joubert syndrome identifies a locus on chromosome 9q34.3 and evidence for genetic heterogeneity. *Am J Hum Genet* **65**: 1666–1671.

Saraiva JM, Baraitser M. 1992. Joubert syndrome: a review. *Am J Med Genet* **43**: 726–731.

Serhatlioglu S, Kocakoc E, Kiris A, Sapmaz E, Boztosun Y, Bozgeyik Z. 2003. Sonographic measurement of the fetal cerebellum, cisterna magna, and cavum septum pellucidum in normal fetuses in the second and third trimesters of pregnancy. *J Clin Ultrasound* **31**: 194–200.

Souka AP, Snijders RJ, Novakov A, Soares W, Nicolaides KH. 1998. Defects and syndromes in chromosomally normal fetuses with increased nuchal translucency thickness at 10–14 weeks of gestation. *Ultrasound Obstet Gynecol* **11**: 391–400.

Steinlin M, Schmid M, Landau K, Boltshauser E. 1997. Follow-up in children with Joubert syndrome. *Neuropediatr* **28**: 204–211.

Valente EM, Salpietro DC, Brancati F, *et al*. 2003. Description, nomenclature, and mapping of a novel cerebello-renal syndrome with the molar tooth malformation. *Am J Hum Genet* **73**: 663–670.

van Dorp DB, Palan A, Kwee ML, Barth PG, van der Harten JJ. 1991. Joubert syndrome: a clinical and pathological description of an affected male and a female fetus from the same sibship. *Am J Med Genet* **40**: 100–104.

van Zalen-Sprock RM, van Vugt JM, van Geijn HP. 1996. First-trimester sonographic detection of neurodevelopmental abnormalities in some single-gene disorders. *Prenat Diagn* **16**: 199–202.

Wang P, Chang FM, Chang CH, Yu CH, Jung YC, Huang CC. 1999. Prenatal diagnosis of Joubert syndrome complicated with encephalocele using two-dimensional and three-dimensional ultrasound. *Ultrasound Obstet Gynecol* **14**: 360–362.

Zalel Y, Seidman DS, Brand N, Lipitz S, Achiron R. 2002. The development of the fetal vermis: an in-utero sonographic evaluation. *Ultrasound Obstet Gynecol* **19**: 136–139.